coatings

MDPI

Article

Plasma Spraying of a Microwave Absorber Coating for an RF Dummy Load

Andreas Killinger [1], Gerd Gantenbein [2], Stefan Illy [2], Tobias Ruess [2], Jörg Weggen [2] and Venancio Martinez-Garcia [1,*]

[1] Institute for Manufacturing Technologies of Ceramic Components and Composites (IMTCCC), University of Stuttgart, Allmandring 7b, 70569 Stuttgart, Germany; andreas.killinger@ifkb.uni-stuttgart.de
[2] Institute for Pulsed Power and Microwave Technology (IHM), Karlsruhe Institute of Technology, Hermann-von-Helmholtz-Platz 1, 76344 Eggenstein-Leopoldshafen, Germany; gerd.gantenbein@kit.edu (G.G.); stefan.illy@kit.edu (S.I.); tobias.ruess@kit.edu (T.R.); joerg.weggen@kit.edu (J.W.)
* Correspondence: venancio.martinez-garcia@ifkb.uni-stuttgart.de

Abstract: The European fusion reactor research facility, called International Thermonuclear Experimental Reactor (ITER), is one of the most challenging projects that involves design and testing of hundreds of separately designed reactor elements and peripheric modules. One of the core elements involved in plasma heating are gyrotrons. They are used as a microwave source in electron–cyclotron resonance heating systems (ECRH) for variable injection of RF power into the plasma ring. In this work, the development and application of an alumina-titania 60/40 mixed oxide ceramic absorber coating on a copper cylinder is described. The cylinder is part of a dummy load used in gyrotron testing and its purpose is to absorb microwave radiation generated by gyrotrons during testing phase. The coating is applied by means of atmospheric plasma spraying (APS). The absorber coating is deposited on the inner diameter of a one-meter cylindrical tube. To ensure homogeneous radiation absorption when the incoming microwave beam is repeatedly scattered along the inner tube surface, the coating shows a varying thickness as a function of the tube length. By this it is ensured that the thermal power is distributed homogeneously on the entire inner tube surface. This paper describes a modeling approach of the coating thickness distribution, the manufacturing concept for the internal plasma spray coating and the coating characterization with regard to coating microstructure and microwave absorption characteristics.

Keywords: microwave; absorber coating; Al_2O_3/TiO_2; APS; 170 GHz; gyrotron; fusion reactor

Citation: Killinger, A.; Gantenbein, G.; Illy, S.; Ruess, T.; Weggen, J.; Martinez-Garcia, V. Plasma Spraying of a Microwave Absorber Coating for an RF Dummy Load. *Coatings* **2021**, *11*, 801. https://doi.org/10.3390/coatings11070801

Academic Editor: Robert B. Heimann

Received: 17 May 2021
Accepted: 25 June 2021
Published: 2 July 2021

1. Introduction

Energy production by means of fusion technology is one of the most ambitious projects that mankind initiated in the last century. The world's largest research facility so far, which is still under construction, is ITER in Cadarache in southern France. Thirty-five nations are collaborating to erect a facility that hopefully proves the feasibility of fusion as a large-scale and carbon-free source of energy [1]. It is based on the so-called tokamak concept that uses a magnetic confinement to heat, compress and hold the plasma in place. Many other research facilities are operated in parallel by international consortia throughout the world. In Germany this is Wendelstein 7-X (W7-X) in Greifswald (stellarator concept) and ASDEX Upgrade in Garching (tokamak concept). The Joint European Torus (JET) in Oxfordshire in UK is another important European research facility. USA, China, Japan, Korea and India are planning or already running their own research centers. However, besides the magnetic confinement principle (tokamak and stellarator), there exist other fusion concepts like inertial confinement that are being developed in parallel.

Fusion technology involves thousands of components that have to be designed and integrated into an overall functionable system. The core components comprise the vacuum torus vessel and several types of superconducting magnetic coils to heat the plasma and keep it in place. Other important components allow for injection of microwaves for plasma heating, as well as components for plasma diagnostics.

Electron–cyclotron resonance heating (ECRH) is one of the main concepts for variable microwave heating of the plasma. Gyrotrons are the main source for the microwave power and are capable of operating in the radio frequency (RF) range of 100–200 GHz with an output power of 1–2 MW. In the case of ITER, they are operated at a frequency of 170 GHz running at a continuous power of 1 MW. In total, 24 gyrotrons will be installed at ITER in the first phase.

A major step in the development and commissioning phase of gyrotrons is extensive testing and conditioning of the device. Stable and reliable RF loads are required to drive the gyrotron to full performance. We report on an RF load with a cylinder, covered with RF absorbing material as the main element.

The development of absorber coatings used in fusion reactor components began in the last decade of the last century. In order to efficiently work as a microwave absorber in the relevant wave length, ceramic coatings with thickness values in a typical range of 100 to 200 µm are required. Resonant coatings in this thickness range can exceed absorption values of 90% for 140 GHz microwave stray radiation [2]. The most important requirements of the ceramic materials are a high dielectric constant, a reasonable high heat conductivity, high resistance against electromagnetic and thermal loads and a good substrate adhesion [2]. Moreover, a high vacuum compatibility is required to minimize outgassing effects induced by the desorption of volatile substances. Nearly all components in fusion reactors that are situated close to the plasma are operated under high or ultrahigh vacuum conditions. Regarding the requested properties and coating thickness range, thermal spraying in general is the technology of choice to apply oxide and some non-oxide coatings. Plasma spraying as the industrial standard, either operated in vacuum (VPS) or under atmospheric conditions (APS), has proven to be a suitable technique to apply ceramic coatings on various metal components (Cu, Mo, Al, Co, carbon, etc.) for this purpose. Most used absorber materials at present are chromium oxide (Cr_2O_3), mixed alumina-titania (Al_2O_3/TiO_2) sprayed using APS and boron carbide (B_4C) sprayed using VPS. Depending of the component, to which the coating is applied, one of these ceramic materials may be favored. For thermally highly loaded devices that are operated close to the plasma ring, an absorber coating with a higher thermal conductivity may be of advantage. As shown in [3], chromium oxide has some benefits in direct comparison to other oxides like alumina-titania or zirconia based coatings. It also exhibits a higher melting point and can withstand high thermal loads without showing any alterations in its microstructure.

An in depth study of the absorption behavior of different APS sprayed oxides ceramic coatings for 140 GHz stray radiation was worked out in [4]. The application in mind was the coating of water-cooled baffle shields that protect cryo-pumps and prevent them from heating up in the microwave stray field of the W7-X fusion reactor in Greifswald. For this purpose, an effective absorber coating was searched. Aluminium oxide, chromium oxide, titanium oxide, zirconium oxide and different mixtures of alumina-titania were evaluated and compared. The study revealed that mixed alumina-titania coatings achieved the highest absorption values of over 90%. However, within different ratios (97/3; 87/13; 60/40), different maximum absorption values were observed, with a 50/50 mixture showing the highest values. Moreover, spray angle and grain size distribution of the initial spray powder also had a tremendous effect of the maximum absorption value.

The development of gyrotrons for W7-X as well as ITER has induced some more efforts to develop absorber coatings, especially for testbed dummy loads, as published in [5]. The paper describes the basic concept for a dummy load design with a mixed aluminum titanium oxide absorption coating. A prototype with a steel tube body was tested successfully. It can be regarded as the technical precursor of the copper tube used in this work. In [6], plasma

sprayed B_4C and Cr_2O_3 as single coatings and mixed bilayer of $Cr_2O_3 \cdot B_4C$ were evaluated for high power loads going up to 1 MW/m^2. The paper discusses advantages and drawbacks of the different materials and emphasizes the importance of a high thermal diffusivity which is best for B_4C, acceptable for Cr_2O_3 but somewhat limited for mixed alumina-titania. VPS also shows superior results if directly compared to APS due to the lower porosity of the coatings. Since then, more work has been published for further improvements of high-power dummy load design capable of collecting radiation power pulses in the range 1–2 MW/m^2. Several research groups from Japan [7,8] presently working at ITER and JT60SA on this subject. Similar effort is still going on to coat bolometers and other highly loaded devices that are operated close to the plasma ring for diagnostic purposes, as described in [9] from a research group working at W7-X.

2. Radio Frequency Technical Requirements and Design Principles

The main design goals for the high-power microwave load under consideration can be summarized as follows:

- The load should be capable of absorbing at least 1.5 MW of microwave power at frequency levels in the range 140 GHz to 170 GHz.
- The back-reflected power from the load has to be as small as possible.
- The distribution of the microwave power on the absorbing area of the load should be as homogenous as possible to avoid the formation of thermal hotspots.
- The mechanical design of the load should be robust and it has to be easy to cool.
- If absorbing coating is applied, both the absorbing material and its connection to the underlying structure should withstand excessive heating and electric arcing events.
- The overall costs for components and manufacturing should be in a reasonable frame.

Figure 1 shows the general concept we used for the design of the load: It is based on a symmetric cylindrical structure, where the microwave beam is axially injected through an input port from one side, scattered by a conical mirror on the opposite site and from there distributed to the coated cylindrical surface by multiple reflections. Tapering of the absorbing ceramic layer on the cylinder allows an adaption and balancing of the power density on the structure to avoid hotspots, especially in the case of the first impact of the scattered microwave beam [5,10]. This requirement implies that the thickness of the layer increases from the mirror side to the input area according to the decreasing microwave power density. Finally, the required local thickness of the layer is determined by microwave absorption measurements (see Section 4.3).

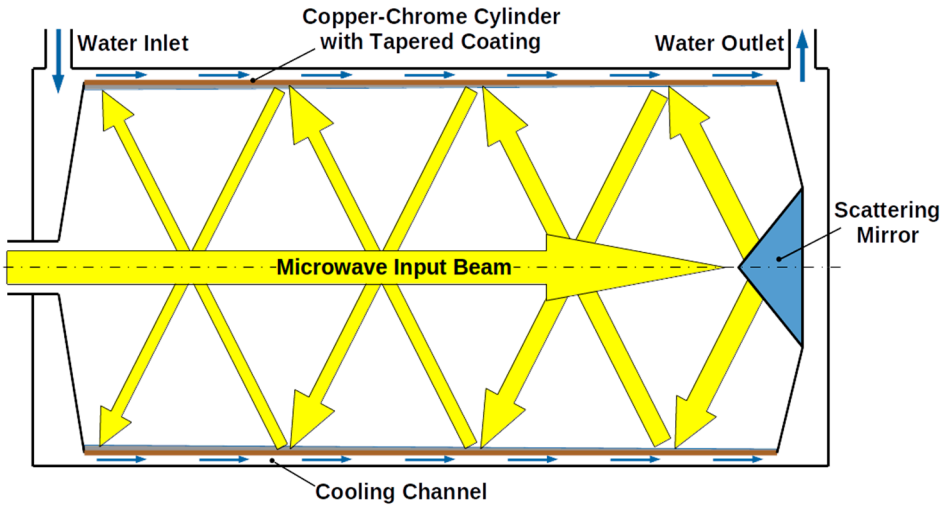

Figure 1. Concept of tube-shaped absorber featuring a microwave absorption layer with a varying coating thickness.

For the design of the load we used a relatively simple "ballistic" ray-tracing code, which even does not take into account the wave diffraction. It simply propagates a larger number of single rays through the geometry, resampling an injected Gaussian beam. At each reflection point, the given power of the ray is reduced according to the assumed absorption coefficient of the respective material until the power of the ray is non-significant or the ray has left the structure through the input port. Figure 2 exemplarily indicates how such a single ray propagates through the geometry, losing its power after multiple reflections. Beside the power density distribution on the internal walls of the load, the code also gives information about the back-reflected power (by integrating the remaining power of all rays leaving the load through the input port).

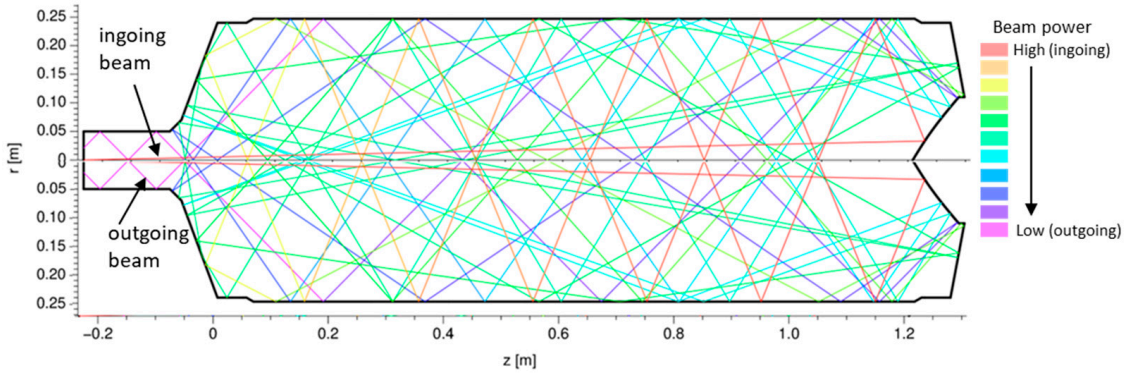

Figure 2. Trace of a single ray starting at the input position (on-axis) with a very shallow angle and propagating through the proposed load geometry. The loss of power is qualitatively indicated by the color (starting from red to magenta, refer to caption on the right side).

While the described simple numerical tool has its limitations, it is sufficient to design and optimize the internal shape of the load, especially the scattering conical mirror. In addition, it allows tuning the variable thickness of the absorbing ceramic layer to avoid excessive values of the power density on the wall, taking into account the measurements of the absorbers described in Section 4.3. Figure 3 shows the expected load profile on the cylindrical part in the case of 1.5 MW injected microwave power at a frequency of 140 GHz in the case of the already optimized design. Each incident beam at the input of the load is assigned a certain power, when this beam hits the circumferential surface of the load, the power is reduced by the absorption coefficient defined at this point. Adding up the losses of the rays gives the power per area. Since none of the peaks exceeds 125 W/cm^2, overheating problems of the thermally well conducting water-cooled copper-chrome structure are not expected [5]. The calculated back-reflected microwave power leaving the load has a value of 2.4% and is therefore easily manageable.

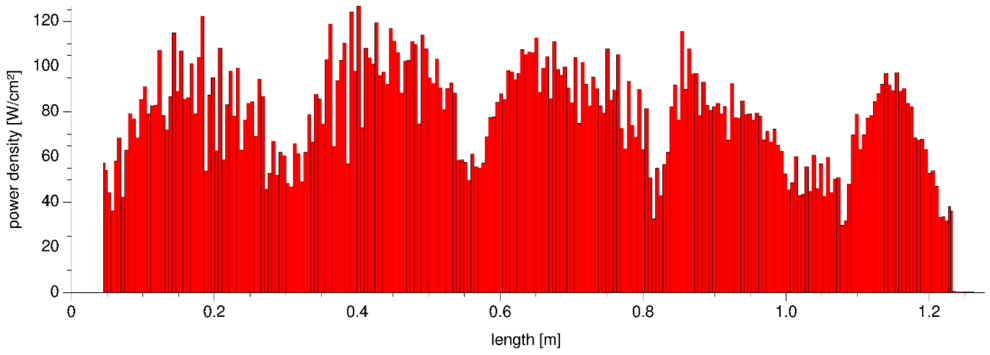

Figure 3. Expected power density on the cylindrical section of the load in the case of 1.5 MW injected power at a frequency of 140 GHz.

3. Materials and Methods

3.1. Copper Collector

The copper collector consists of a tube manufactured by centrifugal casting of a CuCr1-C GZ alloy (DIN 2.1292), with the dimensions summarized in Table 1. Photographs of the tube during preparation are shown in Figure 4.

Table 1. Approximate tube dimensions.

Dimension	Value	Unit
Inner diameter	500	mm
Coating length	1200	mm
Wall thickness	10	mm
Component weight	185	kg

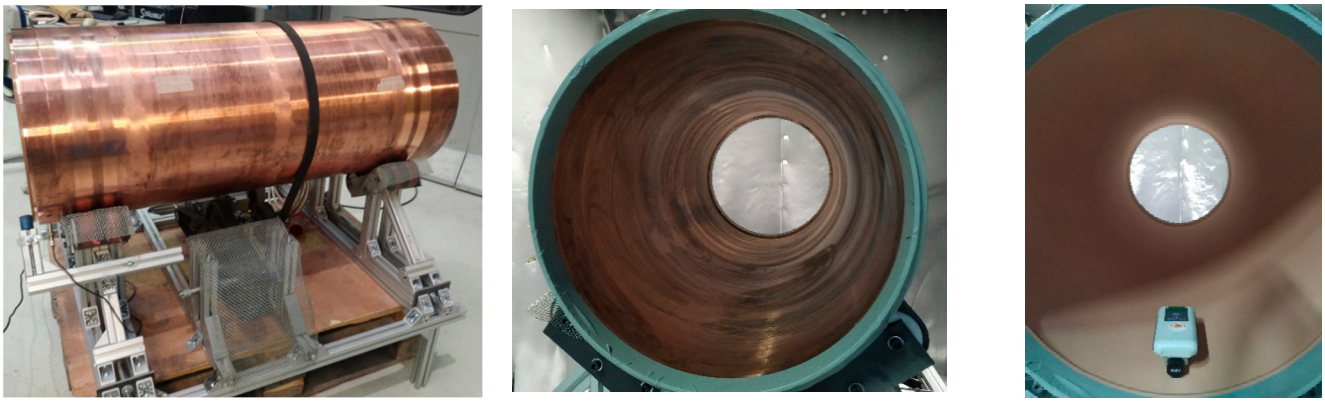

(**a**) (**b**) (**c**)

Figure 4. Tube prior to coating operation, mounted on a rotational support specially constructed for this purpose (**a**). Before sand blasting (**b**) and after (**c**).

The state-of-the-art for internal coatings of cylinders are miniaturized rotating spray torches, in which part is fixed during the coating process and the cylindrical surface is coated by an axial moving and simultaneously rotating torch [11]. This technique is especially applicable for coating of small diameter cylinders, such as cylinder liner surfaces in engine blocks with a diameter of typically 90 mm. However, for larger diameters, the rotation of the tubular part with a synchronized linear movement of the torch is more meaningful. In this case, a handling system is used to position the part exactly under rotation with the centerline of the cylindrical surface [12]. This approach allows for using a standard plasma torch setup operated at optimal spray distance (~150 mm) where the highest particle velocities can be achieved [13]. This way, a dense coating microstructure and optimal coating adhesion can be achieved. To rotate the copper collector, a hand-ling system was designed and constructed, transmitting the rotation with a belt drive, as shown in Figure 5a. The torch is mounted to an extension of the robot system that allows for entering the cylinder and moving in an axial direction synchronously to obtain a 2 mm offset per cylinder revolution, as shown in Figure 5b.

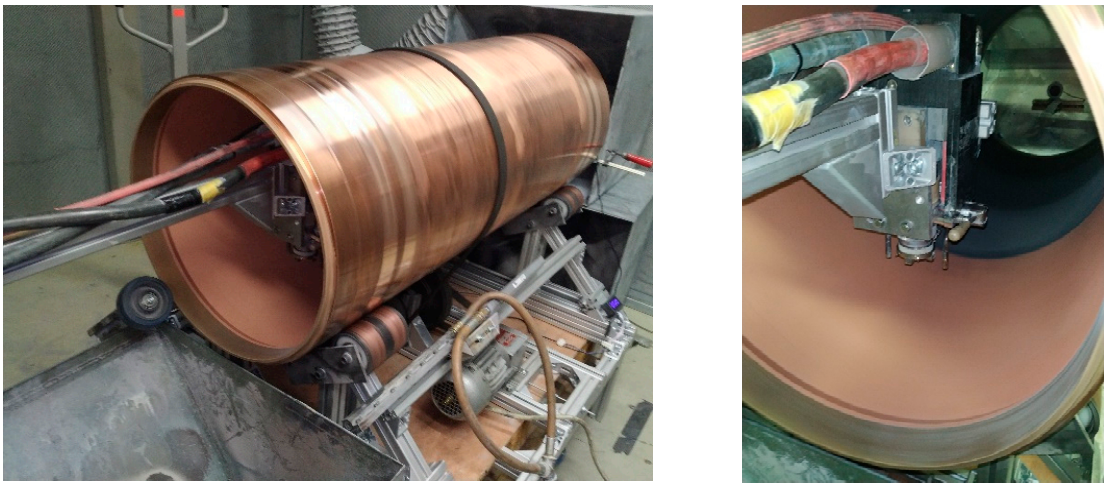

(**a**) (**b**)

Figure 5. Tube prior to coating operation mounted on a rotational support specially constructed for this purpose. A belt drive was designed to set the tube into rotation during coating (**a**). The plasma torch is mounted on a robot-guided cantilever for internal operation. Plasma torch mount shown in more detail in (**b**).

3.2. Powder Feedstock

In a previous work, different oxide coatings were analyzed, revealing that coating thickness, grain size and material composition strongly influence the system absorption [4]. It turned out that Al_2O_3 and TiO_2 mixed powders in different compositions led to higher absorption values compared to pure oxide ceramic materials, with an increasing absorption capability with increasing content of TiO_2. All the spray powders had the same particle size distribution of −20 + 5 µm (prevalent mesh size notation based on ASTM B214 sieve analysis, referring to a particle size distribution of D_{10} = 5 and D_{90} = 20, respectively). The coating thickness was fixed to 150 µm [4].

The selected spray powder by consideration of previous works is an Al_2O_3/TiO_2 60/40 mixture for APS coatings supplied by Oerlikon Metco AG (Pfäffikon, Switzerland), with the characteristics summarized in Table 2.

Table 2. Oxide ceramic Spray Powder. Given are manufacturer's data.

Manufacturer	Designation	Composition	Particle Size (µm)
Oerlikon Metco AG	Amdry 6250	60% Al_2O_3, 40% TiO_2	D10 = 5 µm D90 = 35 µm

3.3. Coating Deposition and Characterization

Atmospheric plasma spraying was performed using a standard F6 type plasma gun from GTV GmbH (Luckenbach, Germany). The spray torch was guided by a six-axis robot system type RX130B from Stäubli International AG (Pfäffikon, Switzerland). Plasma parameters were adjusted in order to achieve a well adherent and dense coating structure. Powder feed rate was adjusted to achieve a suitable coating thickness in the range of 15 µm per spray pass using a PF962 powder feeder from GTV GmbH (Luckenbach, Germany). The coating thickness per past is adjusted by modifying the amount of powder injected during the process adjusting the rotation speed of the feed disc. The optimized spray parameters that were finally applied for coating operation are summarized in Table 3.

Surface activation of the inner tube surface has been done by bead blasting with glass beads (300 µm) and degreased using acetone before and after the bead blasting process in order to enhance the mechanical adhesion of the coating to the substrate. The considerably soft material had to be treated carefully to avoid implantation of the bead particles and therefor this operation was performed using a reduced air pressure of 2 bar. A surface

roughness with Ra 5.3 µm and Rz 40 µm was achieved. Surface roughness was measured using a contact profilometer type Perthometer Concept from Mahr GmbH (Göttingen, Germany), Rz and Ra values were determined according to DIN EN ISO 4287.

Table 3. Optimized spray plasma spray parameter set used in coating operation of the tube.

Parameter	Symbol	Value	Unit
Plasma gun current	I	500	A
Plasma gun voltage	V	75	V
Plasma gun power	P	37,5	kW
Plasma gas mixture	$\dot{V}_{Argon}$	44	l/min
	$\dot{V}_{H2}$	10	l/min
Powder feed gas	$\dot{V}_{Argon}$	8	l/min
Spray distance	h	130	mm
Torch transversal speed [1]	v	500	mm/s
Meander offset	b	3	mm
Rotational speed	ω	20	r.p.m
Cooling nozzles distance	d	65–70	mm

[1] Torch transversal speed measured relative to the moving substrate surface.

The particle size distribution of the Al_2O_3/TiO_2 60/40 mixture powder was determined by means of laser diffraction particle size analysis in a Mastersizer S from Malvern Panalytical Ltd. (Malvern, United Kingdom) in order to ensure the powder specifications. The material was investigated by scanning electronic microscopy (SEM); the sample was sputter-coated with gold and examined in a LEO VP 438 from Leo Elektronenmikroskopie GmbH (Oberkochen, Germany).

Prior to spraying on the tube component, testing of the spray process was performed on flat samples that were mounted inside a dummy tube with the same diameter to be coated under similar conditions as the absorber coating. This way, a comparable spray process situation like that on the real component is guaranteed. Test samples of CuCrZr copper alloy (formerly CuCrZr), with discs geometry of 124 mm diameter and 8 mm thickness, were coated and used for coating characterization regarding absorption. Coating characterization was done by metallographic cross section preparation and optical micrograph images of the coatings were performed using a Leica MEF4M (Leica GmbH, Wetzlar, Germany) as well as SEM micrographs.

The coating thickness is determined in the copper collector by non-destructible methods, using a portable contact system DUALSCOPE® FMP100 coating thickness gauge from Helmut-Fischer GmbH (Germany), which uses the eddy current testing method (DIN EN ISO 2360) for non-ferrous metals. Temperature measurements during the coating process were performed using an IR pyrometer type Optris CTlaser LTF-SF-CB8 from Micro-Epsilon Messtechnik GmbH & Co. KG. (Ortenburg, Germany).

The bond strength was measured according to the pull-off method ISO 14916 with a measuring device on a universal testing machine Zwick Z100 from ZwickRoell GmbH & Co. KG (Ulm, Germany). HTK ULTRA BOND® from HTK Hamburg GmbH (Hamburg, Germany) was used as adhesive and pins with a diameter of 14.2 mm were used as tension rods. Precipitation heat treatment of the glue took place at 190 °C for 35 min. The test speed was set to 0.5 mm/min. The phase composition of APS coatings and spray powder was investigated using the Advance D8 diffractometer from Bruker Corporation (Billerica, MA, USA) with a Cu Kα beam and a graphite monochromator.

Microwave absorption measurements were performed on flat sample coatings as-sprayed with different thicknesses from 30 µm to 150 µm at 140 GHz and 170 GHz. A schematic view of the reflection measurement setup is shown Figure 6 [14]. A millimeter (mm)-wave is transmitted by a corrugated circular horn antenna. The mm-wave is focused on the dielectric coated samples using two mirrors. The reflected signal is separated from the forwarding transmission path using a Mylar foil at 45° angle. The reflected signal is received by a corrugated circular horn antenna and is evaluated by a

performance network analyzer (PNA). The frequency range of the PNA is limited up to 26.5 GHz and is increased using extension modules, covering the frequency band from 140–220 GHz.

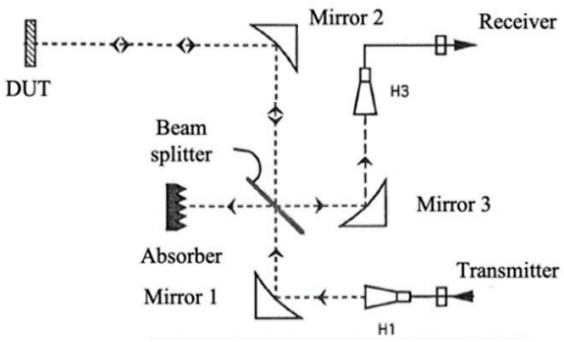

Figure 6. Schematic view of the mm-wave absorption measurement setup for coated disks [14].

4. Results

4.1. Powder Characterization

The particle size distribution analysis of the APS powder for quality control is summarized in Figure 7a. The grain size distribution curve exhibits micrometer-sized particles with D10 = 8 µm, D50 = 17 µm and D90 = 33 µm. The particle size distribution represents a monomodal distribution. There was no significant fine fraction nor agglomerates in the delivered powder. The analysis of the SEM images is in accordance with the results of the laser granulometry, showing irregularly shaped particles, as can be seen from Figure 7b.

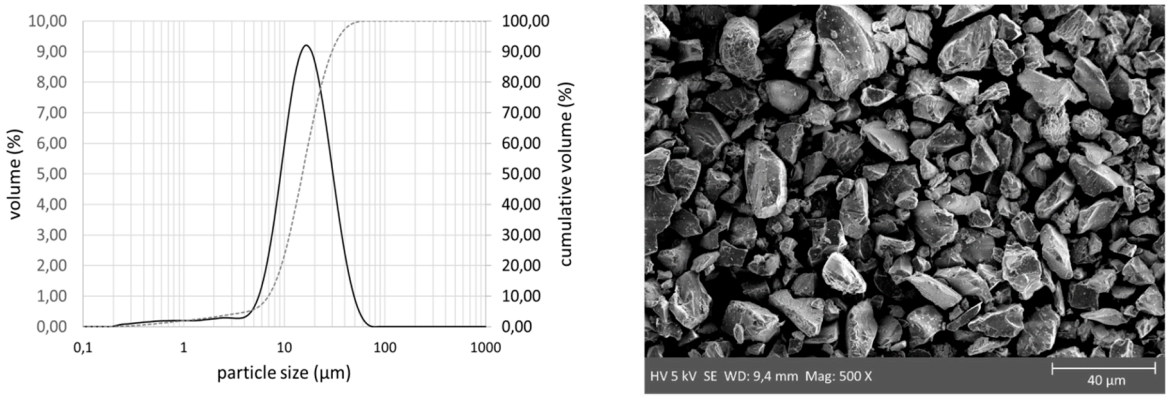

(**a**) (**b**)

Figure 7. Laser granulometry (**a**) and scanning electron microscope image (**b**) of the alumina-titania spray powder.

4.2. Structural and Microstructural Properties of the Deposited Coatings on Flat Samples

In a first step, flat copper discs (CuCr1Zr copper alloy; 124 mm in diameter and 8 mm in thickness) were spray-coated employing a meander movement. These samples were then used for evaluation and coating characterization regarding their absorption ability as a function of varying thickness starting from 30 µm to 150 µm (i.e., 30, 45, 60, 75, 100, 125 and 150 µm), obtaining the same coating characteristics, such as microstructure and porosity.

Inside the tube, environmental conditions are strongly affected by plasma gas and cooling gas flows. These strongly differ from a corresponding outside coating process. To mimic the coating conditions that predominate inside the copper tube, a second series of copper disks were then mounted and coated inside a dummy steel tube refer to Figure 8a with the same dimensions as the final copper tube, as shown in Figure 8b. As described below, the optimal thickness range to coat the final copper tube was selected from 50 µm to

100 μm (i.e., 50, 60, 75, 90 and 100 μm), according to the simulations presented in Section 2 and the MW absorption measurements on Section 4.3.

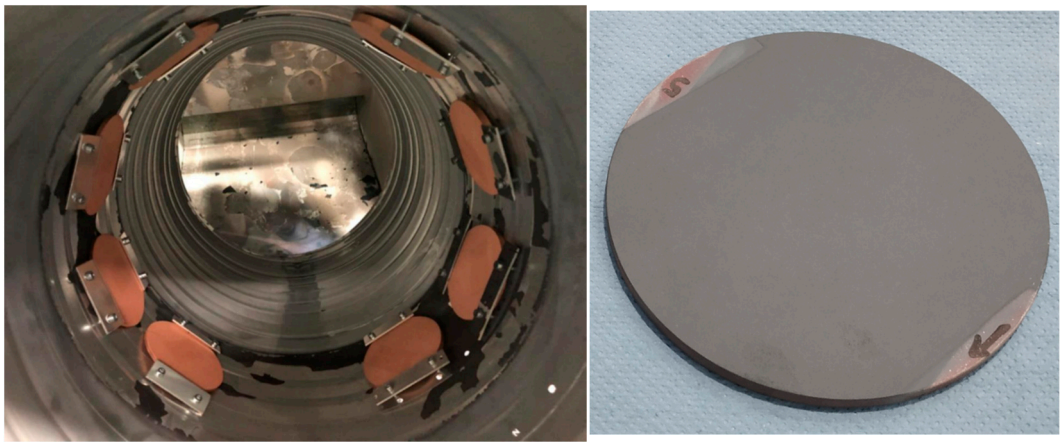

(**a**) (**b**)

Figure 8. Test samples mounted in dummy steel tube prior to plasma spray coating operation (**a**). Planar test sample after plasma spray deposition of the oxide ceramic (**b**). See more details in text.

These samples were also characterized by means of microscopic image analysis of coating cross sections and by the eddy current testing method. Figure 9 shows an example of the coating microstructure that was achieved under internal coating conditions with a 100 μm coating thickness. The copper particles that can be found within coating are due to preparative restraints during cross section polishing treatment. In the optical microscope image, shown in Figure 9a, and SEM images, shown in Figure 9b, dark areas represent Al_2O_3 rich phases, whereas bright areas represent TiO_2 rich phases and stoichiometric solid solution of Al_2O_3 and TiO_2 [15].

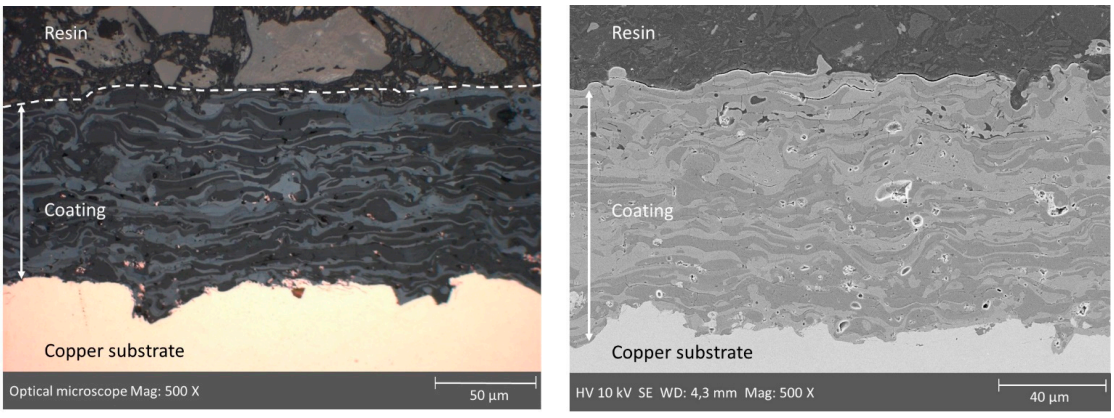

(**a**) (**b**)

Figure 9. Microscopic images of coating cross-sections in optical microscope (**a**) and SEM (**b**). Some copper particles can be found within the ceramic coating near the interface. This happens due to the polishing process during cross-section preparation.

X-ray diffraction (XRD) patterns acquired on the as-deposited coatings and spray powder, shown in Figure 10, lead to the conclusion that the coatings deposited by APS have phase composition of γ–Al_2O_3, aluminium titanate (Al_2TiO_5) and rutile TiO_2 as main constituents. It is well known that, due to the high cooling rates, a major fraction of α–Al_2O_3 of the initial phase is converted γ–Al_2O_3 during the spray process. Aluminium titanate (Al_2TiO_5) is also formed during the spray coating process. A smaller quantity of α–Al_2O_3 and anatase TiO_2 is also visible in the pattern [16]. The bond strength analysis

shows values of 9.67 ± 0.83 MPa with adhesive fracture mode, which are consistent with the results obtained in other works [4,17].

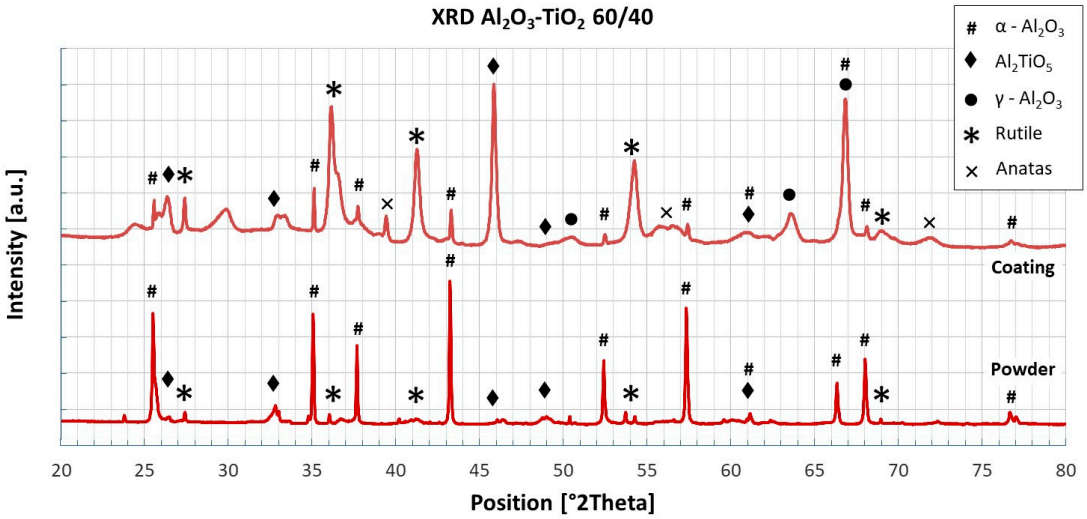

Figure 10. XRD patterns of the as-sprayed APS Al_2O_3/TiO_2 60/40 coating (upper) and spray powder (lower).

4.3. Microwave Absorption Measurements on Flat Samples

The microwave absorption measurement results of the coated samples with Al_2O_3/TiO_2 60/40 at 140 GHz and 170 GHz are shown in Figure 11. In addition, previous measurements with a mixture of Al_2O_3/TiO_2 87/13 at 140 GHz are depicted [4]. In each measurement, the resonance is clearly visible at which an absorption maximum is reached. The resonance occurs when the thickness t corresponds to $\lambda_m/4$, where λ_m is the wavelength in the medium, given by Equation (1):

$$t = \frac{\lambda_m}{4} = \frac{\lambda_0}{4 \cdot \sqrt{\epsilon_r}} = \frac{c_0}{4 \cdot f \cdot \sqrt{\epsilon_r}}. \quad (1)$$

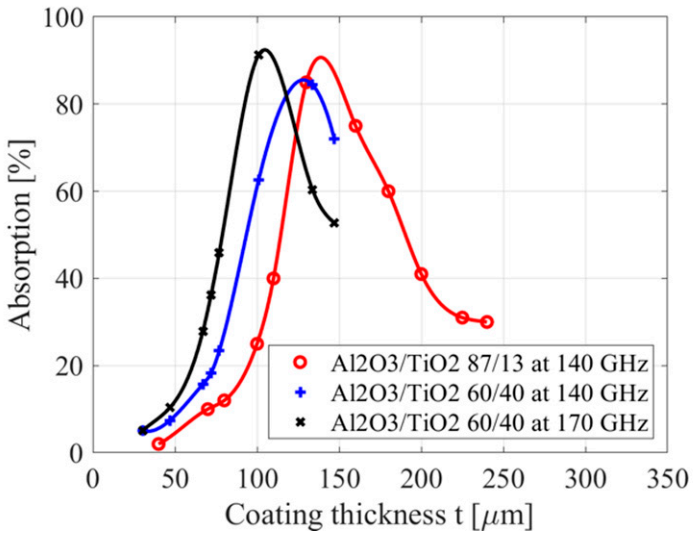

Figure 11. Comparison of the absorption measurements of Al_2O_3/TiO_2 87/13 at 140 GHz (red curve) [4] and Al_2O_3/TiO_2 60/40 at 140 GHz (blue curve) and at 170 GHz (black curve).

The resonance condition is dependent on the frequency f and the relative permittivity ϵ_r. In particular, the amount of TiO_2 affects the dielectric properties of the composite because of its very high relative permittivity of $\epsilon_r \approx 169$ at 140 GHz [18]. The relative permittivity of Al_2O3/TiO_2 60/40 is calculated to be $\epsilon_r \approx 17.5$, in contrast to $\epsilon_r \approx 14.8$ of the 87/13 mixture. Changing the relative permittivity of the mixture affects the resonance condition, as shown in Figure 11, which directly changes the absorption of the coating thicknesses. In addition, the absorption of the coating at 170 GHz is higher compared to 140 GHz up to a coating thickness of ≈ 110 µm.

4.4. Coating of the Copper Dummy Load

The copper dummy load was coated in different steps to obtain the specified coating thickness distribution in different lengths from 50 µm to 100 µm (i.e., 50, 60, 75, 90 and 100 µm). The thickness distribution relative to the position in the collector was determined non-destructively using the DUALSCOPE® FMP100 from Helmut Fischer GmbH (Sindelfingen, Germany) coating thickness gauge. The obtained coating distribution is measured in increments of 20 mm. For each measuring position in the axial direction, four points circumferentially distributed are determined to calculate the mean value and standard deviation, as shown in Figure 12. The maximum coating thickness tolerances for the application are specified in ±10 µm. To represent the good stability of the coating process and the high accuracy of the coating thickness, the tolerance limits shown are specified in ±5 µm.

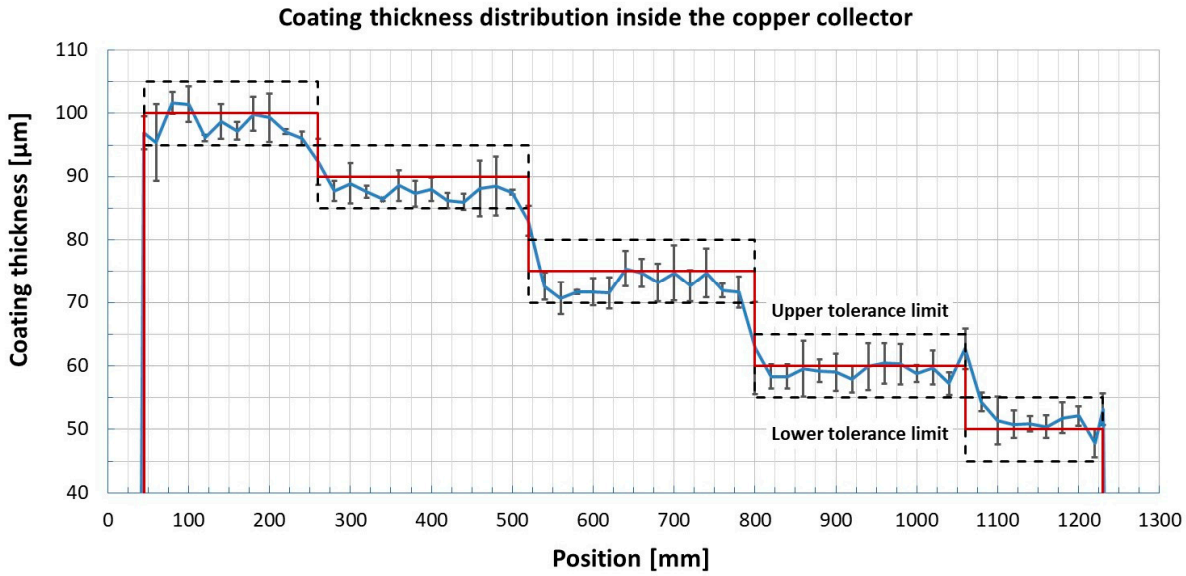

Figure 12. Coating thickness distribution measurement (blue line) of the coated copper collector; also shown are desired values of coating thickness (red line) and tolerance limits (black dotted lines).

4.5. Results from High Power Tests with a 1 MW Gyrotron

The load was tested with a 1 MW 170 GHz gyrotron in short and long pulses up to quasi continuous wave operation. The experiments were performed at the KIT gyrotron test stand. For full power operation (~1 MW) the maximum pulse length is limited to 180 s due to limitations in the power supply of the gyrotron, for lower power (~500 kW) longer pulses are possible. The applied flow rate for the examples given below was 700–750 L/min.

Figure 13a shows the temperature behavior of the cooling water during a pulse of 180 s duration and an average power deposition of 800 kW. In the first part and after the end of the pulse an oscillation of the temperature is visible. In order to have correct calorimetry both oscillations have to be taken into account. This is due to the closed-loop cooling system and is not related to the operation of the gyrotron or the load. Due to optimization of the operating parameters, the gyrotron power increases during the pulse. This allows to

calculate the instantaneous power at the end of the pulse from the temperature value to be more than 900 kW, with still increasing tendency.

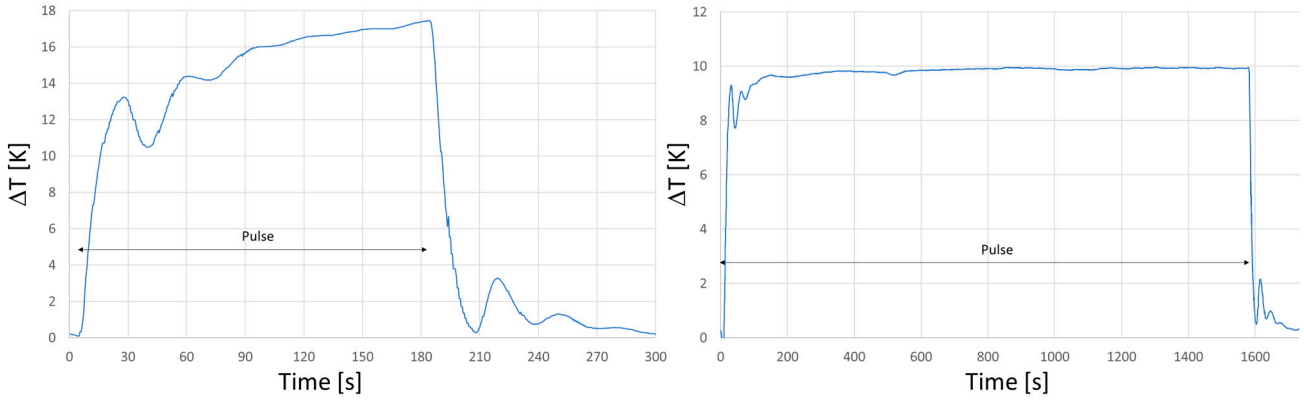

Figure 13. Cooling water temperature during a shot with 180 s pulse duration (**a**). Cooling water temperature during a shot with 1571 s pulse duration (**b**).

Very long pulses with a duration of up to 26 min were performed with an RF power of approximately 500 kW. Figure 13b shows a 1572 s pulse, where operating parameters were not modified during the pulse. It is visible that after 200 s the water temperature is stable, indicating a constant output power of the gyrotron.

In general, the behavior of the load was very good during the experiments. Arcing in the load, which is a frequent problem in such operations, was very much limited and did not slow down the experimental progress. Visual inspection of the load after the first experimental phase did not reveal any defects.

5. Discussion

Several challenges had to be overcome when applying the internal absorber coating on the dummy load. Realization of a variable coating thickness as a function of the tube length needs some preliminary studies to learn more about the spray conditions that control deposition rate and efficiency as well as coating morphology, i.e., porosity and phase composition inside the tube. These properties are not necessarily the same if compared to coatings produced on small samples under regular conditions. Besides, the manufacturing of an internal coating especially demands a sophisticated temperature guidance by using air lances close to the plasma torch for the internal cooling and additional air knives for outside cooling of the tube surface.

For calibration purposes, test samples have to be manufactured, preferably showing comparable coating properties. With these data in hand, a correlation function of thickness and absorption values can then be derived.

We therefore decided to fabricate the flat samples inside a steel tube to mimic similar process conditions. The cooling concept had to be adapted, as the heat flow of the massive copper tube is much more effective than it is the case in the separated flat copper samples mounted inside the steel tube. During the coating of flat samples, the dummy steel tube reached a maximum temperature of between 120 and 170 °C and the copper samples temperatures between 100 and 130 °C. During the coating of the copper tube, the tube reached a maximum temperature of between 50 and 60 °C. In principle, this has to be taken into account when directly comparing deposition efficiencies and resulting coating thickness during the plasma spray process. On the other hand, the overall temperature levels reached in the process were quite low (100 to 120 °C and 50 to 60 °C, respectively) therefore we do not expect to see strong differences in coating thickness.

Finally, for implementation of a variable coating thickness in the copper tube, several approaches are possible. A continuous change of the coating thickness values could basically be realized by a successive adjustment of the transfer speed of the plasma torch during the coating process. Indeed, this would have made necessary several trials on dummy tubes to exactly work out and adjust the torch and tube kinematic to meet the claimed thickness distribution function. In the present case this was not feasible due to existing cost and time restrictions. The stepwise application of layered coatings therefore represents a good compromise between economic viability and technical requirements. Moreover, this approach is scalable and adjustable to almost any size and thickness gradations.

6. Conclusions

The application of an absorber coating with varying thickness into a copper dummy load was successfully conducted in three steps. First, the estimation of the optimal thickness distribution of the coating as a function of the tube length was calculated from raytracing simulation of the microwave beam. In a second step, planar copper samples where coated in varying thickness to achieve the absorption as a function of the coating thickness for plasma sprayed Al_2O_3/TiO_2 60/40. From this calibration, the coating thickness distribution in the tube could then be calculated. It turned out, that a stepwise alteration of the thickness was sufficient for the task and was much easier to realize in the manufacturing process.

Careful simulations of the power loading of a high-power RF absorber load with a ray-tracing code have shown that the device can handle up to 1.5 MW without exceeding the maximum allowable power density limits. Several low-power microwave measurements at different frequencies were performed in order to define the optimum absorption and thickness of the layer to get a preferably homogeneous power distribution. These measurements verified the optimum thickness variation along the axis in the order of 50 to 100 um. In the first phase of experiments, the load was operated successfully with a power in the order of 800–900 kW (limited by the available gyrotron). Up to now no limitations of the load have been observed. In the near future it is planned to use this load with a 1.5 MW gyrotron.

Author Contributions: Conceptualization, V.M.-G., A.K., and G.G. conceived and designed the experiments; V.M.-G. made the samples, V.M.-G., S.I., and T.R. performed the experiments; V.M.-G., A.K., S.I., T.R., and J.W. analyzed the data; V.M.-G. technical construction for coatings; V.M.-G., A.K., and G.G. wrote the paper. All authors critically reviewed the content and approved final version for publication. All authors have read and agreed to the published version of the manuscript.

Funding: This research received no external funding.

Institutional Review Board Statement: Not applicable.

Informed Consent Statement: Not applicable.

Acknowledgments: We would like to thank Andreas Eigenthaler from the Institute for Manufacturing Technologies of Ceramic Components and Composites in Stuttgart for his help with the technical construction and preparation of the samples. We thank Willi Schwan from IFKB at University of Stuttgart for his support in sample preparation and microscope analysis.

Conflicts of Interest: The authors declare no conflict of interest.

References

1. Bigot, B. ITER: A unique international collaboration to harness the power of the stars. *Comptes Rendus Phys.* **2017**, *18*, 367–371. [CrossRef]
2. Wacker, R.; Leuterer, F.; Wagner, D.; Hailer, H.; Kasparek, W. Characterization of absorber materials for high-power millimetre waves. In Proceedings of the Twenty Seventh International Conference on Infrared and Millimeter Waves, San Diego, CA, USA, 26 September 2002; pp. 159–160.
3. Spinicchia, N.; Angella, G.; Benocci, R.; Bruschi, A.; Cremona, A.; Gittini, G.; Nardone, A.; Signorelli, E.; Vassallo, E. Study of plasma sprayed ceramic coatings for high power density microwave loads. *Surf. Coat. Technol.* **2005**, *200*, 1151–1154. [CrossRef]
4. Floristán, M.; Müller, P.; Gebhardt, A.; Killinger, A.; Gadow, R.; Cardella, A.; Li, C.; Stadler, R.; Zangl, G.; Hirsch, M.; et al. Development and testing of 140GHz absorber coatings for the water baffle of W7-X cryopumps. *Fusion Eng. Des.* **2011**, *86*, 1847–1850. [CrossRef]

5. Schmid, M.; Erckmann, V.; Gantenbein, G.; Illy, S.; Kern, S.; Lievin, C.; Samartsev, A.; Schlaich, A.; Rzesnicki, T.; Thumm, M. Technical developments at the KIT gyrotron test facility. *Fusion Eng. Des.* **2011**, *86*, 518–521. [CrossRef]
6. Bin, W.; Bruschi, A.; Cirant, S.; Muzzini, V.; Simonetto, A.; Spinicchia, N.; Angella, G.; Dell'Era, F.; Gantenbein, G.; Leonhardt, W.; et al. Absorbing coatings for high power millimeter-wave devices and matched loads. *Fusion Eng. Des.* **2013**, *88*, 2510–2514. [CrossRef]
7. Ioki, K.; Hiranai, S.; Moriyama, S.; Tanaka, S. Development of a dummy load and waveguide components for 1 MW CW gyrotron. *Fusion Eng. Des.* **2016**, *109–111*, 951–955. [CrossRef]
8. Igami, H.; Kubo, S.; Shimozuma, T.; Yoshimura, Y.; Takahashi, H.; Tsujimura, T.I. Development of a quick-response microwave bolometer for the stray radiation measurement in LHD. In Proceedings of the 2018 43rd International Conference on Infrared, Millimeter, and Terahertz Waves (IRMMW-THz), Nagoya, Japan, 9–14 September 2018; pp. 1–2.
9. Marsen, S.; Corre, Y.; Laqua, H.P.; Moncada, V.; Moseev, D.; Niemann, H.; Preynas, M.; Stange, T.; The W7-X Team. First results from protective ECRH diagnostics for Wendelstein 7-X. *Nucl. Fusion* **2017**, *57*, 1–7. [CrossRef]
10. Ives, L.; Mizuhara, M.; Kobayashi, T.; Moriyama, S.; Collins, G.; Borchard, P.; Neilson, J. Design and operation of a 2-MW CW RF load for gyrotrons. *IEEE Trans. Electron Devices* **2014**, *61*, 1800–1805. [CrossRef]
11. Barbezat, G. The state of the art of the internal plasma spraying on cylinder bore in AlSi cast alloys. *Int. J. Automot. Technol.* **2001**, *2*, 47–52.
12. Killinger, A.; Gadow, R.; Buchmann, M.; López, D. Method and Device for Coating the Interior of Hollow Areas by Thermal Injection. PCT Patent WO 2004/005575 A2, 14 January 2004.
13. Gadow, R.; López, D.; Candel, A. Ceramic and Cermet coatings for cylinder liner in ultralightweight engines-novel processing and manufacturing of ceramic layer composites. *Adv. Sci. Tech.* **2006**, *45*, 1330–1335. [CrossRef]
14. Ruess, T.; Gantenbein, G.; Ioannidis, Z.; Rzesnicki, T.; Wagner, D.; Thumm, M.; Jelonnek, J. Frequency measurement techniques for megawatt-class gyrotrons. *Gruyter J.* **2021**. under review.
15. Zhou, J.; Sun, K.; Huang, S.; Cai, W.; Wei, Y.; Meng, L.; Hu, Z.; Li, W. Fabrication and property evaluation of the Al_2O_3-TiO_2 composite coatings prepared by plasma spray. *Coatings* **2020**, *10*, 1122. [CrossRef]
16. Ahn, J.; Hwang, B.; Song, E.P.; Lee, S.; Kim, N.J. Correlation of microstructure and wear resistance of Al_2O_3-TiO_2 coatings plasma sprayed with nanopowders. *Met. Mater. Trans. A* **2006**, *37*, 1851–1861. [CrossRef]
17. Vicent, M.; Bannier, E.; Benavente, R.; Salvador, M.; Molina, T.; Moreno, R.; Sánchez, E. Influence of the feedstock characteristics on the microstructure and properties of Al_2O_3–TiO_2 plasma-sprayed coatings. *Surf. Coat. Technol.* **2013**, *220*, 74–79. [CrossRef]
18. Schermer, R.T.; Stievater, T.H. Millimeter-wave dielectric properties of highly refractive single crystals characterized by waveguide cavity resonance. *IEEE Trans. Microw. Theory Tech.* **2019**, *67*, 1078–1087. [CrossRef]